3) Micropilot Plant Reactor System

The purpose of the Micropilot Plant Reactor system described in Section III B.4. was to analyze the product distributions obtained over Schulz-Floryian and non-Schulz Floryian catalysts obtained under widely variant opearting conditions. As certain bifunctional catalysts such as ZSM-5 contain both a Schulz-Flory type transition metal plus a zeolite function, it was also important to determine from the product distribution, the effect of each component. The family of curves describing the product distributions possible under Schulz-Flory kinetics is shown in Figure 64. Varying the polymerization probability of the Schulz-Flory distribution function derived in Section II C.1. from 15% to 95%, the product distributions predicted by the Schulz Flory model were plotted. At low polymerization probability light gases account for the majority of the product fraction. As the polymerization probability is increased to 95%, the product yield is skewed toward the production of heavy waxes. It was desirable to determine what is the maximum possible C_6 to C_{12} gasoline fraction which could be achieved by conventional Fischer-Tropsch catalysts operating under Schulz-Floryian kinetics. The variation in gasoline fraction with polymerization was modelled and the results are presented in Figure 65. The maximum possible gasoline yield is 42.27%

Figure 64. Family of Curves Describing Schulz-Flory Kinetics

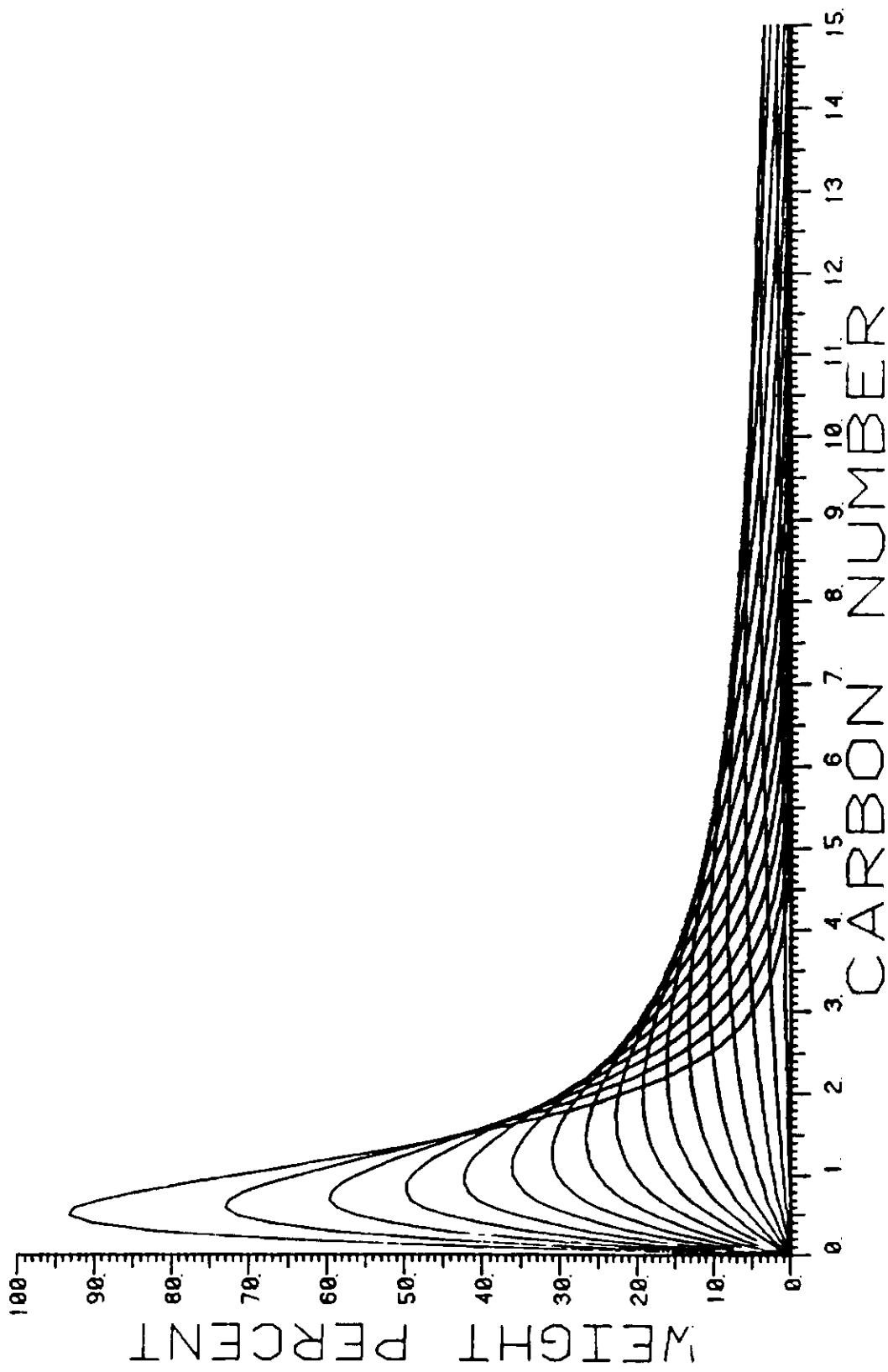

Figure 65. Variation in Gasoline Fraction With Polymerization.

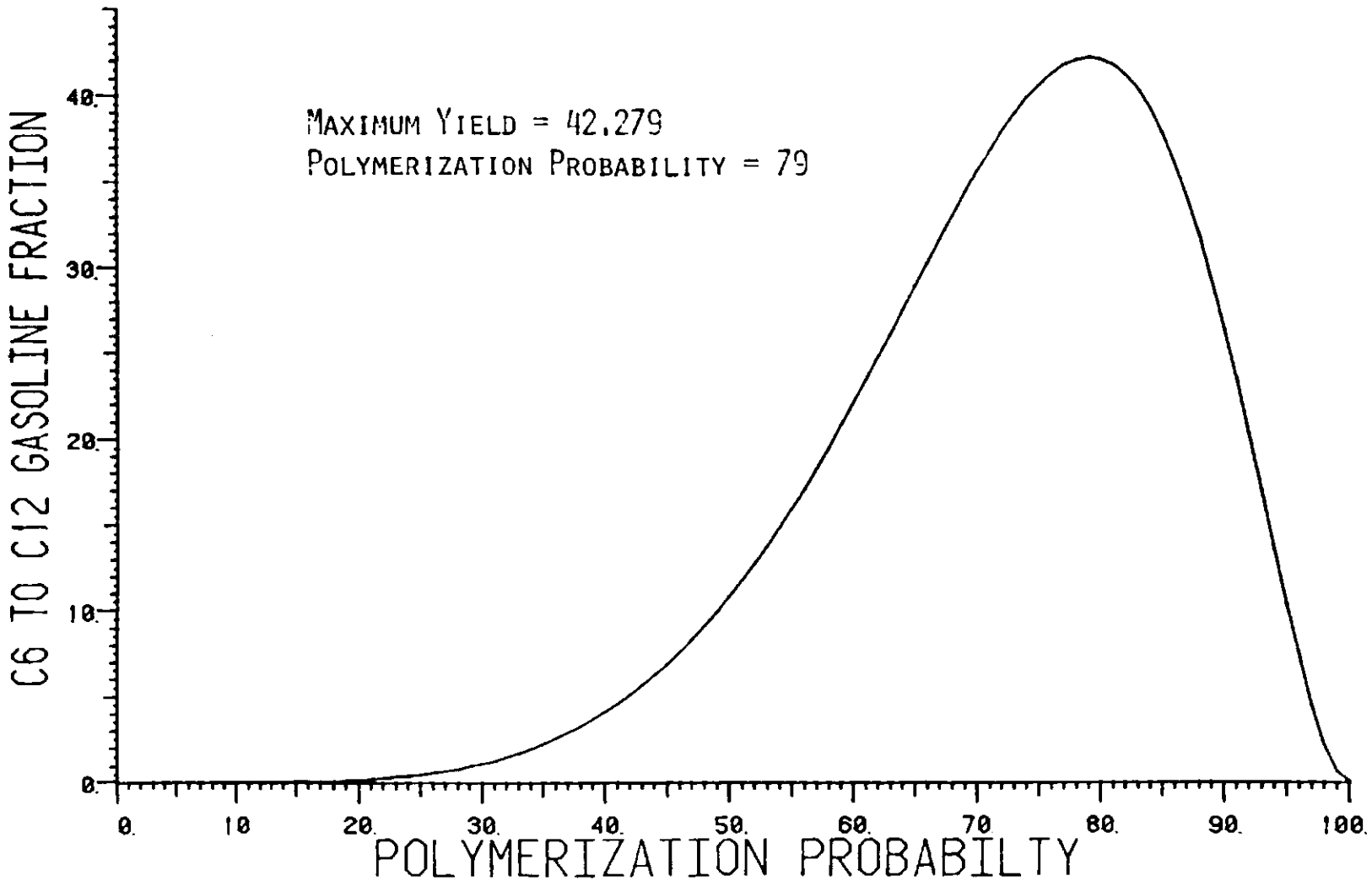

and could be obtained if it were possible to operate the reactor under conditions which would yield an optimum polymerization probability of 79%. Typically, the polymerization probability achieved in commerical plants fall well below 79%. If, however, by increasing pressure, decreasing the synthesis gas ratio, and decreasing temperature a 79% polymerization probability could be achieved, the product distribution containing the maximum possible gasoline fraction would be that shown in Figure 66. It is evident from Figure 66 that even when the gasoline yield is optimized a substantial amount of the product is in the C_1 to C_5 hydrocarbon range and in the C_{13}^+ range. The inherent poor selectivity of Fischer-Tropsch catalysts in gasoline synthesis presents the need for bifunctional shape selective catalysts. When the zeolite function is added it is difficult to determine the effectiveness of each function of a dual function catalyst and its effect on the product distribution. Where the polymerization probability could be used in conjunction with the Schulz-Flory distribution function to determine the product distribution formed on the transition metal, no parameter existed which could be used to scale the effectiveness of the zeolite function. A Pentasil Factor was defined for this purpose.

Figure 66. Product Distribution Containing The Maximum Possible Gasoline Fraction.

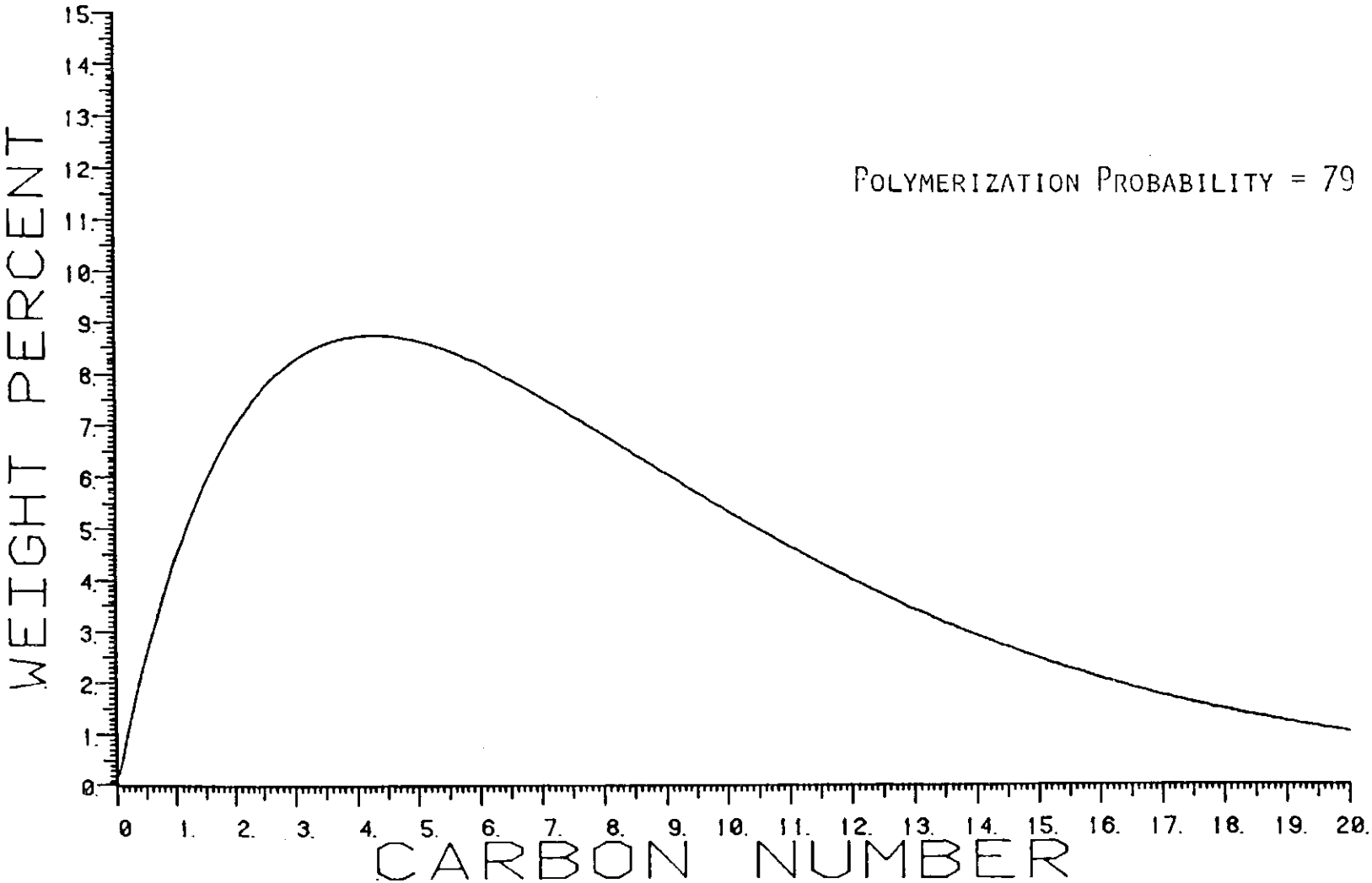

$$\text{Pentasil Factor} = \frac{\text{(The measured gasoline weight fraction - the gasoline weight fraction predicted by the Schulz-Flory distribution function on a methane yield basis)}}{\text{The measured gasoline weight fraction}}$$

If it is assumed that no methane is produced by the cracking activity of ZSM-5 and it is assumed that the methane yield adequately predicts the polymerization probability, this Pentasil Factor can be used to describe what fraction of the gasoline yield is attributable to the ZSM-5 catalyst. As can be seen in Figures 67 and 68 neither the ethane or propane yield uniquely defines the polymerization probability. For all but three points, a specific ethane yield could result from two possible polymerization probabilities. For methane, however, there is a monotonic decrease in methane yield with polymerization probability as is shown in Figure 69. Once the computer in the gas chromatograph has evaluated the product fraction occurring at each carbon number, the LSI-11/23 models the contribution of the Fischer-Tropsch metal by fitting the polymerization probability to the methane yield. The retention times of the normal alkanes are used to assign chromatographic peaks to a particular carbon number. The analysis report shown in Figure 70 is the typical output form for the micropilot plant reactor. The catalyst used was a cobalt thoria catalyst provided by Pittsburgh Energy Technology Center. The reactor operating conditions are shown

Figure 67. Ethane Yield Does Not Define The Polymerization Probability

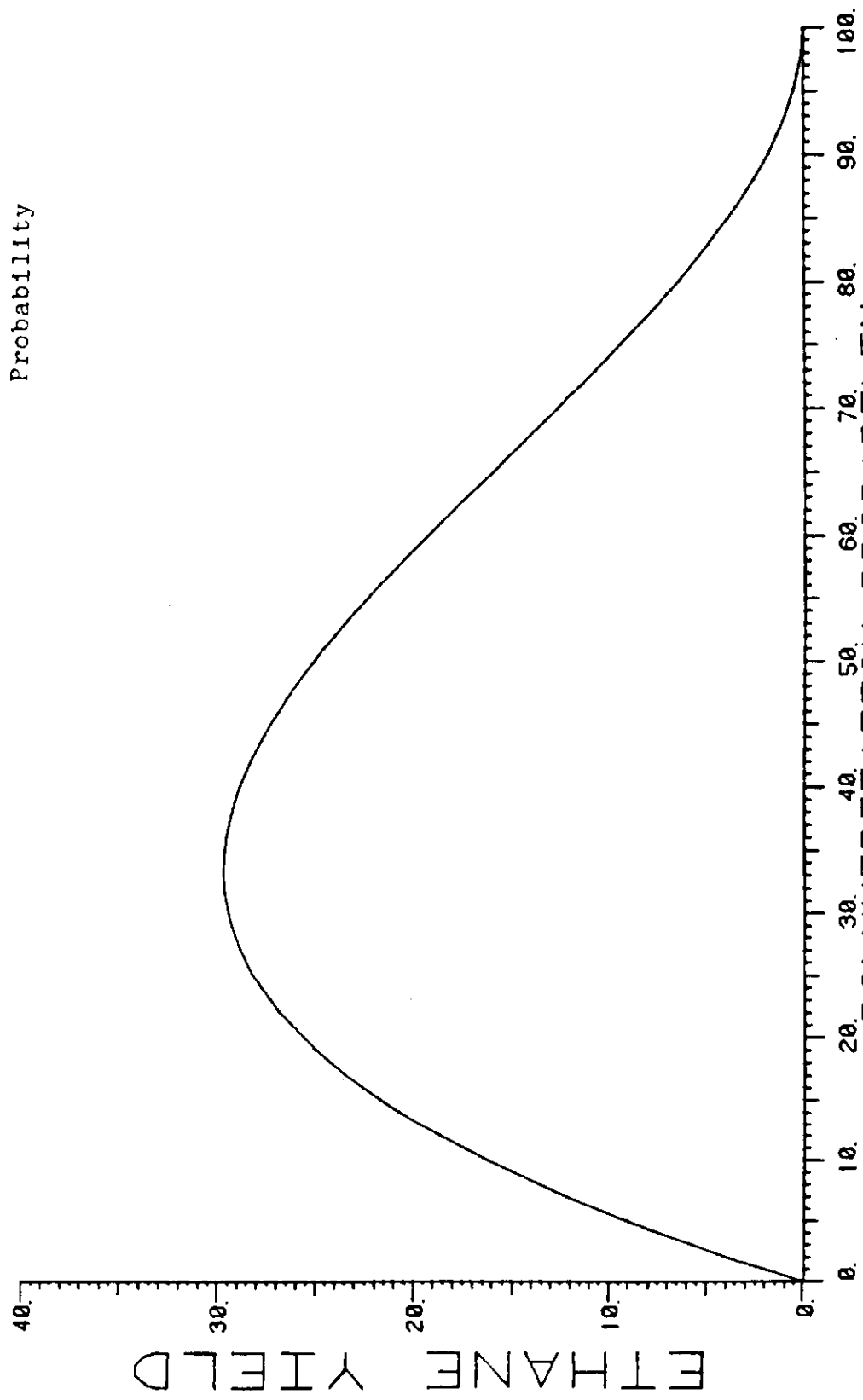

Figure 68. Propane Yield Does Not Define Polymerization Probability.

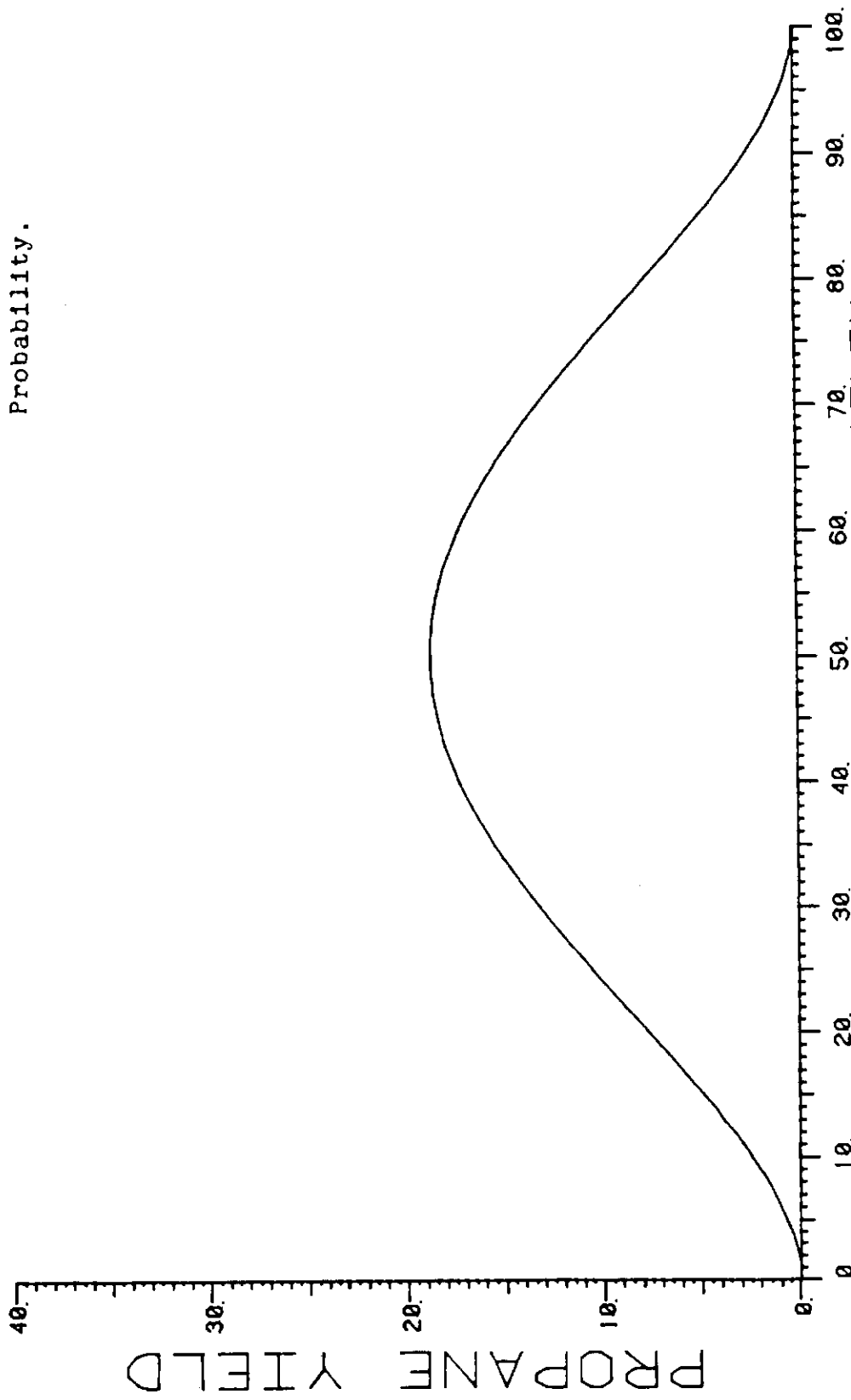

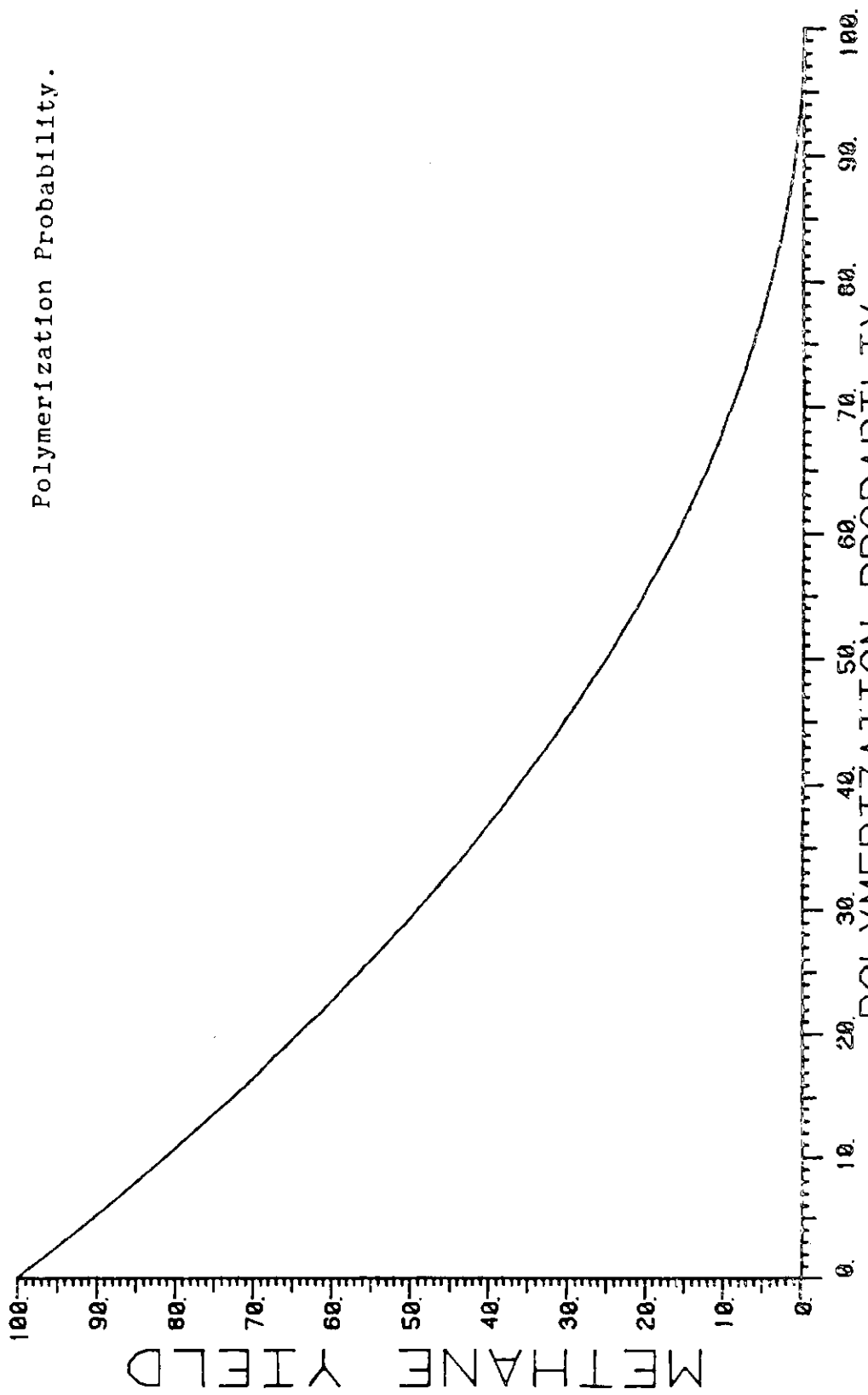

Figure 69. Methane Shows a Monotonic Decrease in Methane Yield with Polymerization Probability.

Figure 70. Typical Output Form for the Micropilot Plant Reactor.

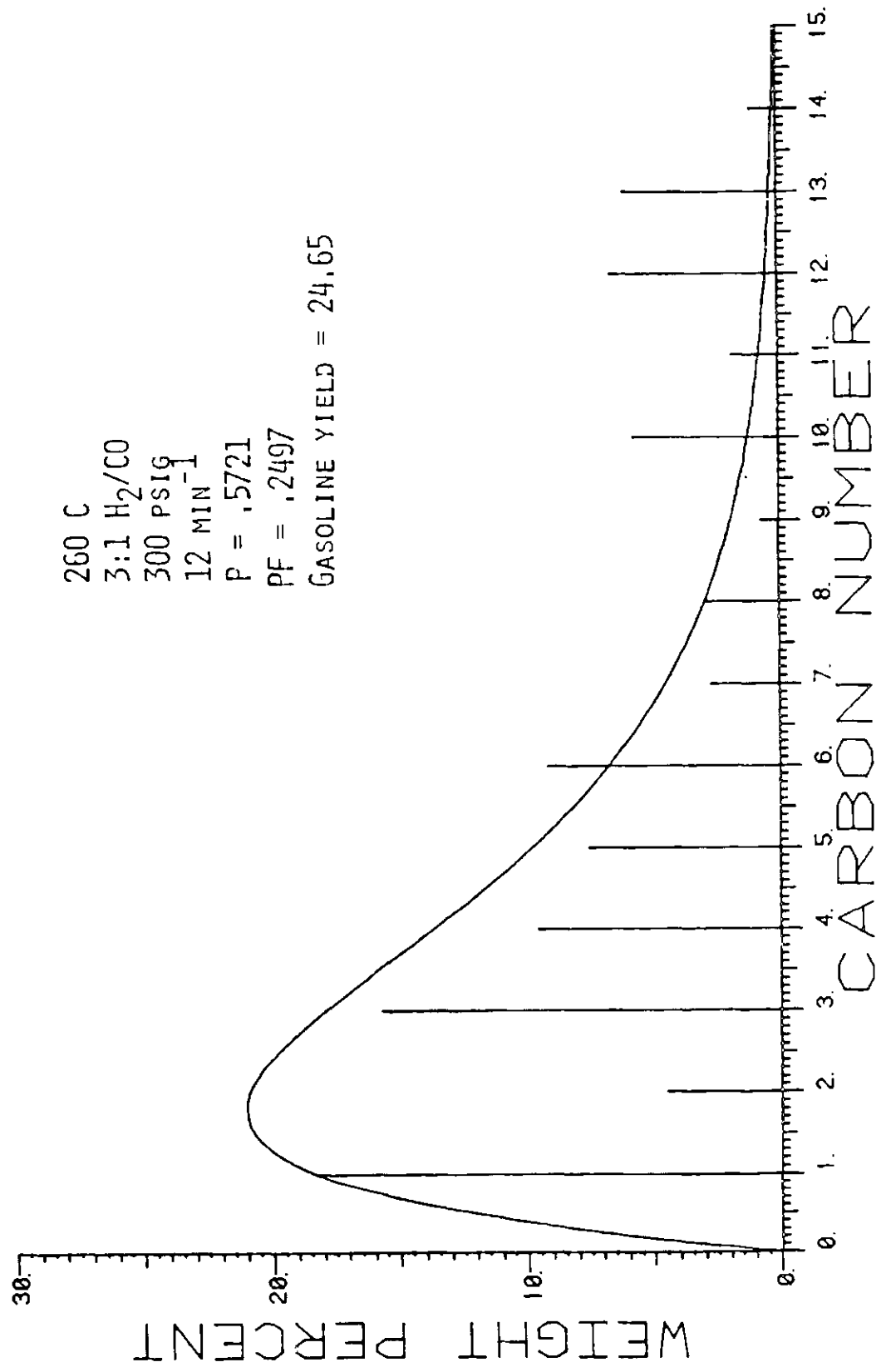

in the Figure. The reactor system determined the gasoline yield to be 24%, the polymerization probability 57%, and the Pentasil Factor occurred because ZSM-5 activity is poor at 260 C. The Schulz-Floryian curve models the product distribution which would have been obtained in the absence of the zeolite catalyst. The vertical lines are a histogram of the actual measured product distribution.

Using the same catalyst and increasing the reaction temperature 10 C.resulted in the product distribution shown in Figure 71. As would be expected, raising the temperature caused a decrease in the polymerization probability. The Pentasil Factor rose from 24% to 68% showing the ZSM-5 catalyst was considerably more effective in increasing the gasoline fraction. The gasoline yield rose to 27%. The sharp cut-off at C_{10} demonstrates the shape selectivity of ZSM-5 and the low fraction of C_2 hydrocarbons is indicative of cobalt catalysts.

The micropilot plant system is a closed loop system enabling the operator to chose the reactor operating conditions through the Tektronix terminal and receive the modelled output approximately an hour later.

Figure 71. Same Catalyst after Increasing Temperature Caused a Decrease in Polymerization Probability.

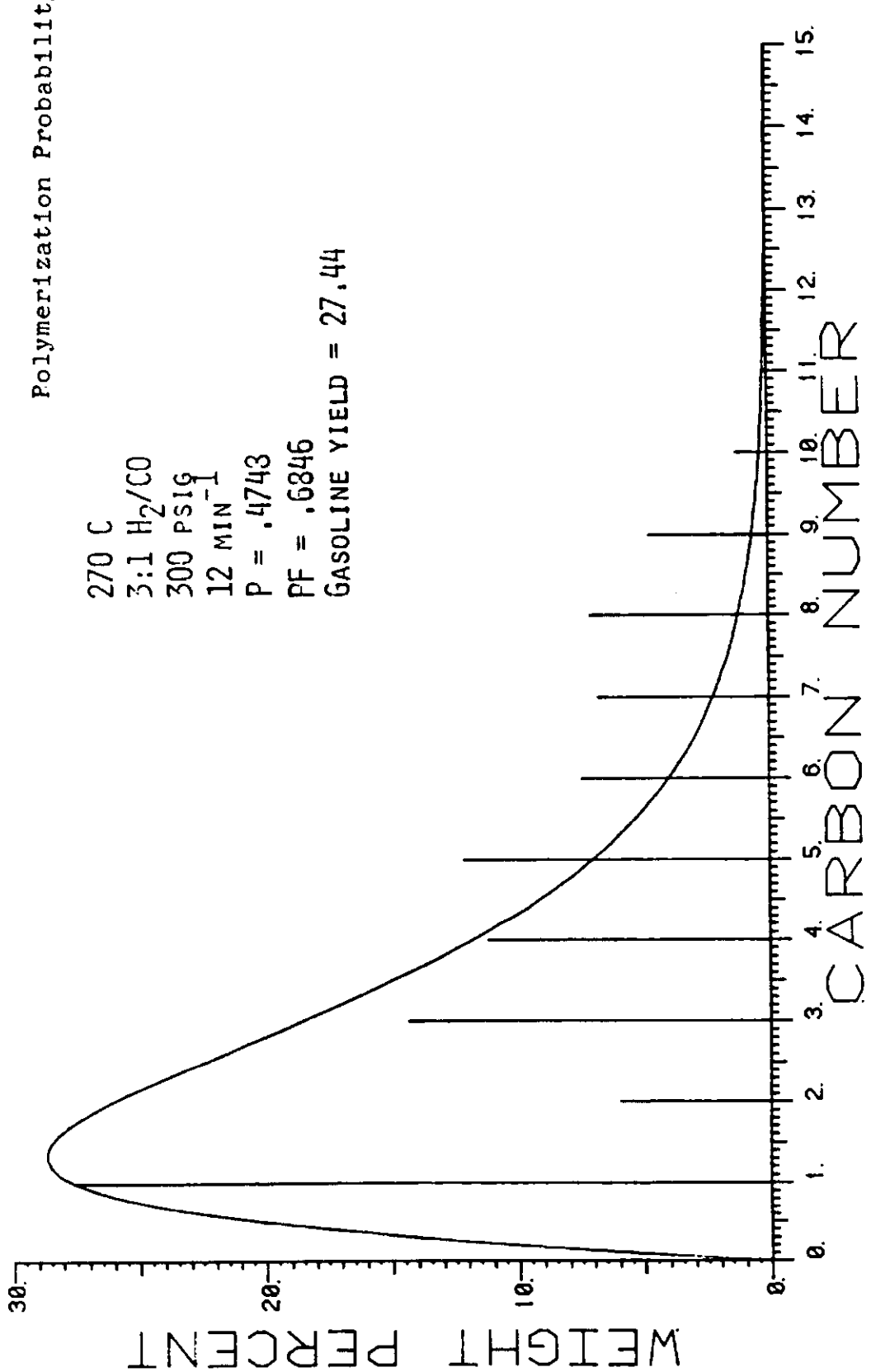

B. Bifunctional Transition-Metal Zeolite Catalysts

1. Synthesis of Nu-5

The synthesis of Nu-5 was carried out in accordance with the procedure described in Example 1 of the ICI European patent application 0054386. The synthesis batch had the molar composition 2.39 Na_2O, 20 pentaerythritol, Al_2O_3, 89 SiO_2, 3600 H_2O, 15.9 SiO_4^{2-}. The rate of crystallization was considerably slower than reported and a reaction time of approximately 96 hours was required to obtain a maximum yield of Nu-5. Quartz and tridymite were major competitive phases in this synthesis at 180 C and can likely be eliminated by lowering the temperature of reaction, lowering the pH of the batch or both. The XRD pattern of the typical product obtained is shown in Figure 72 (λ = 1.5405). The line at 26.67 degrees 2θ demonstrates the presence of the quartz contaminant. Scanning electron micrographs of the Nu-5 product obtained are shown in Figure 73 e,f,g,h.

Further exploratory phase chemistry will be required to obtain Nu-5 of high purity at a desired crystallite size. Literature XRD line patterns for Nu-5 as synthesized, quartz, and tridymite are provided in Figures 74,75, and 76, respectively, for reference. The reported XRD pattern for Nu-5 (Figure 74) is extremely similar to that reported for ZSM-5 (Figure 77). The lesser sorption capacity for m-xylene

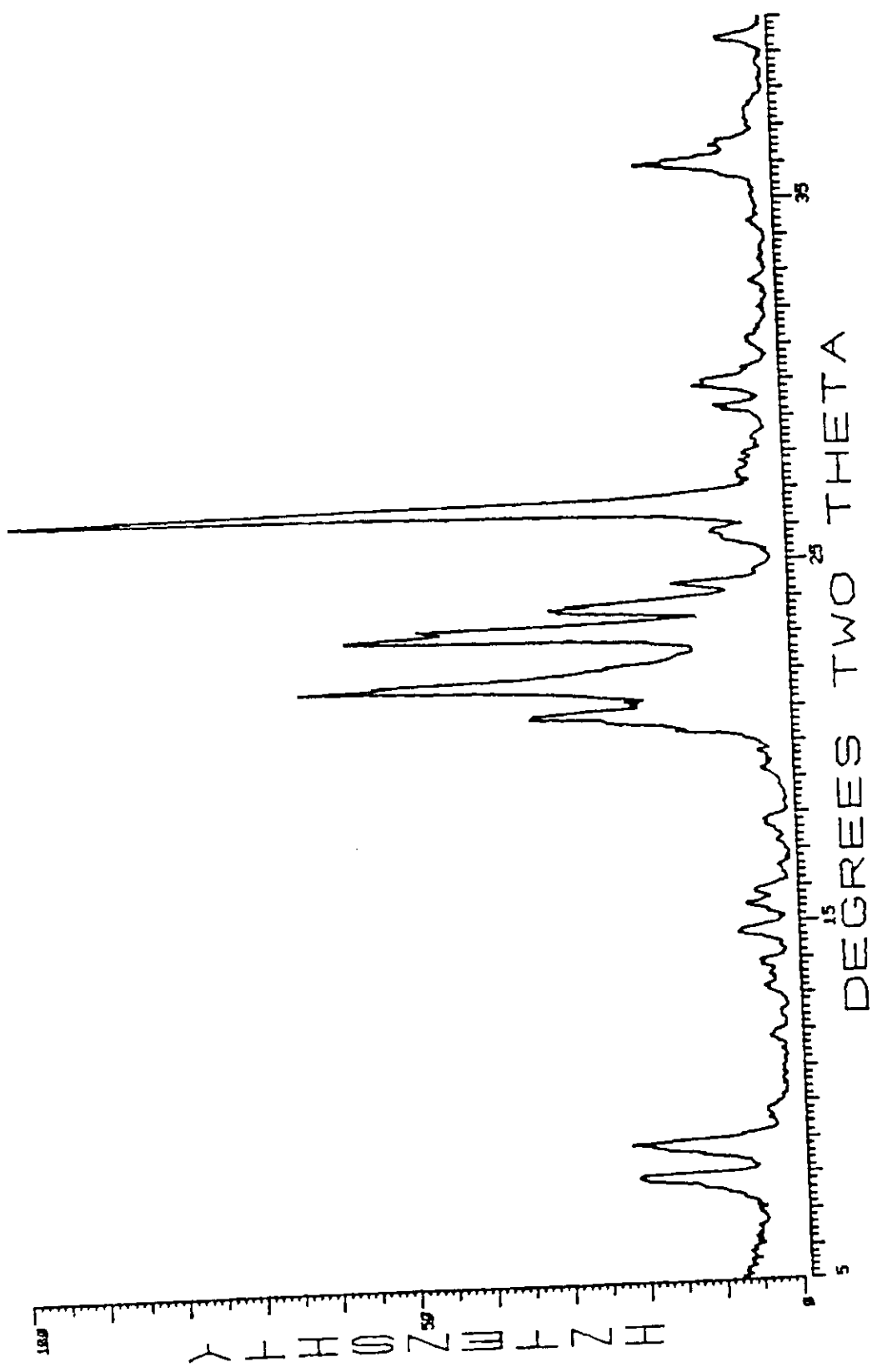

Figure 72. XRD Pattern of Na, Penta erythritol Nu-5

Figure 73. e,f,g,h . Scanning Electron Micrographs of the Nu-5 Product Obtained

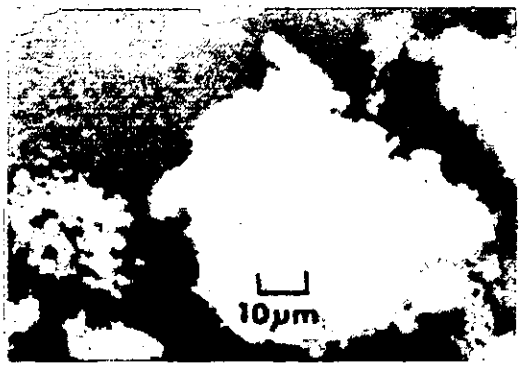

Figure 73 a

Figure 73 b

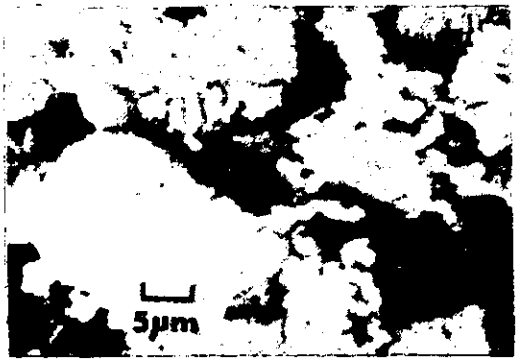

Figure 73 c

Figure 73 d

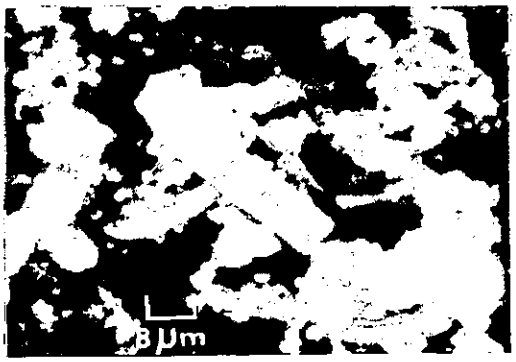

Figure 73 e

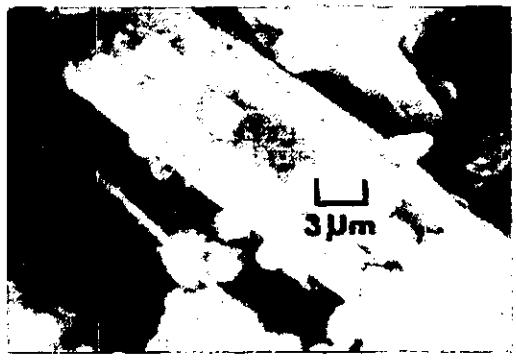

Figure 73 f

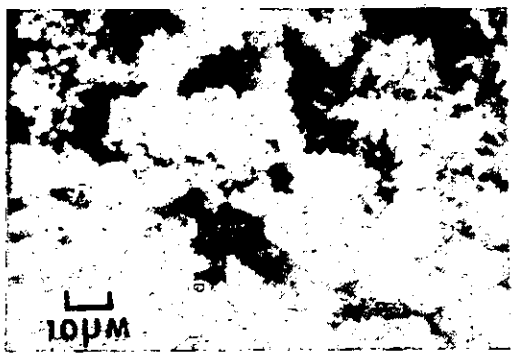

Figure 73 g

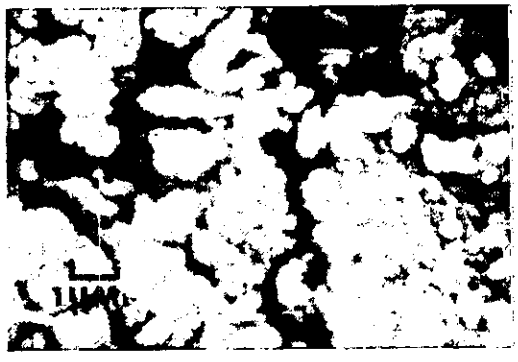

Figure 73 h

Figure 74. XRD Literature Line Pattern for Nu-5 as Synthesized.

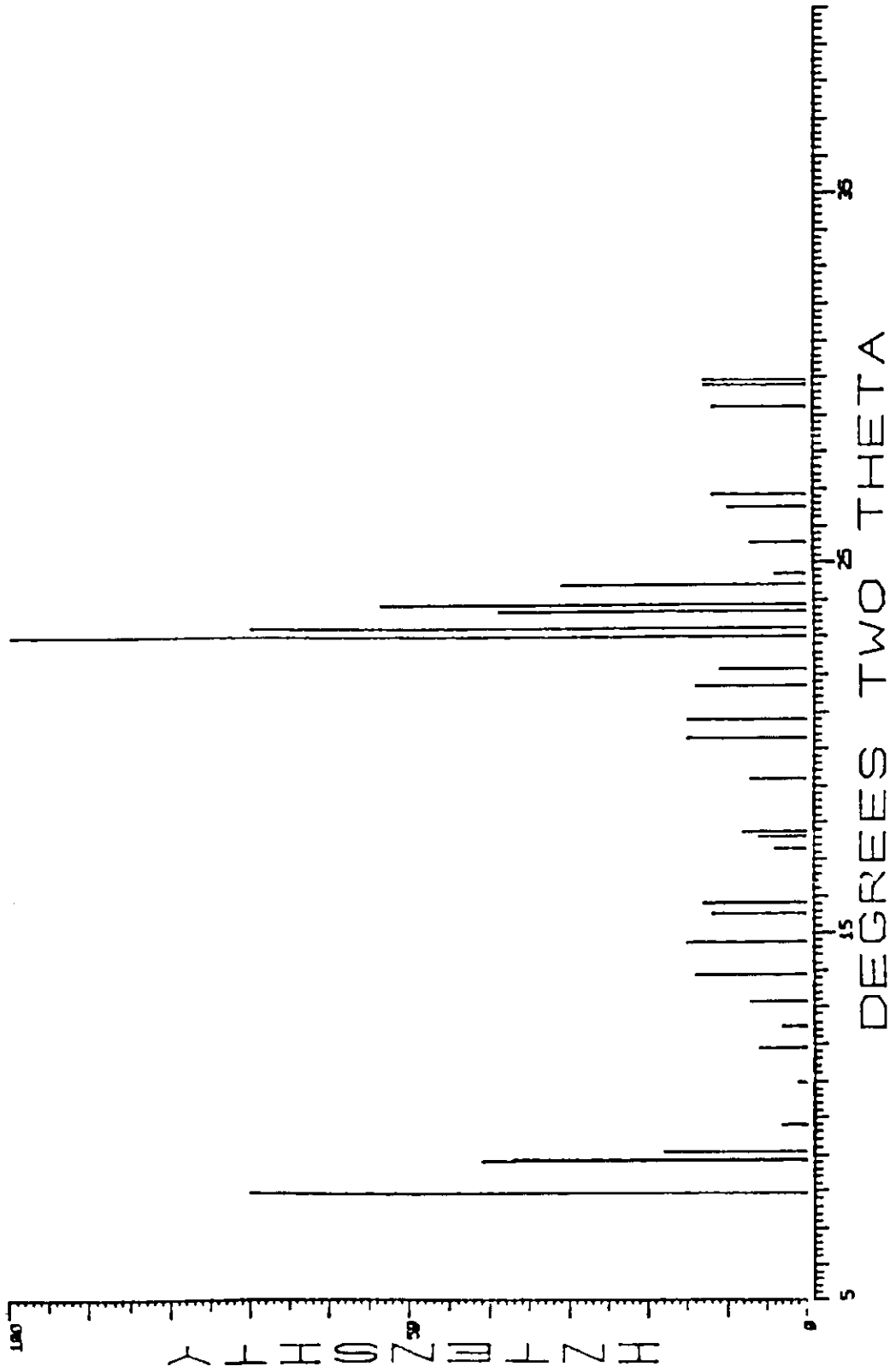

Figure 75. XRD Literature Line Pattern

For Quartz

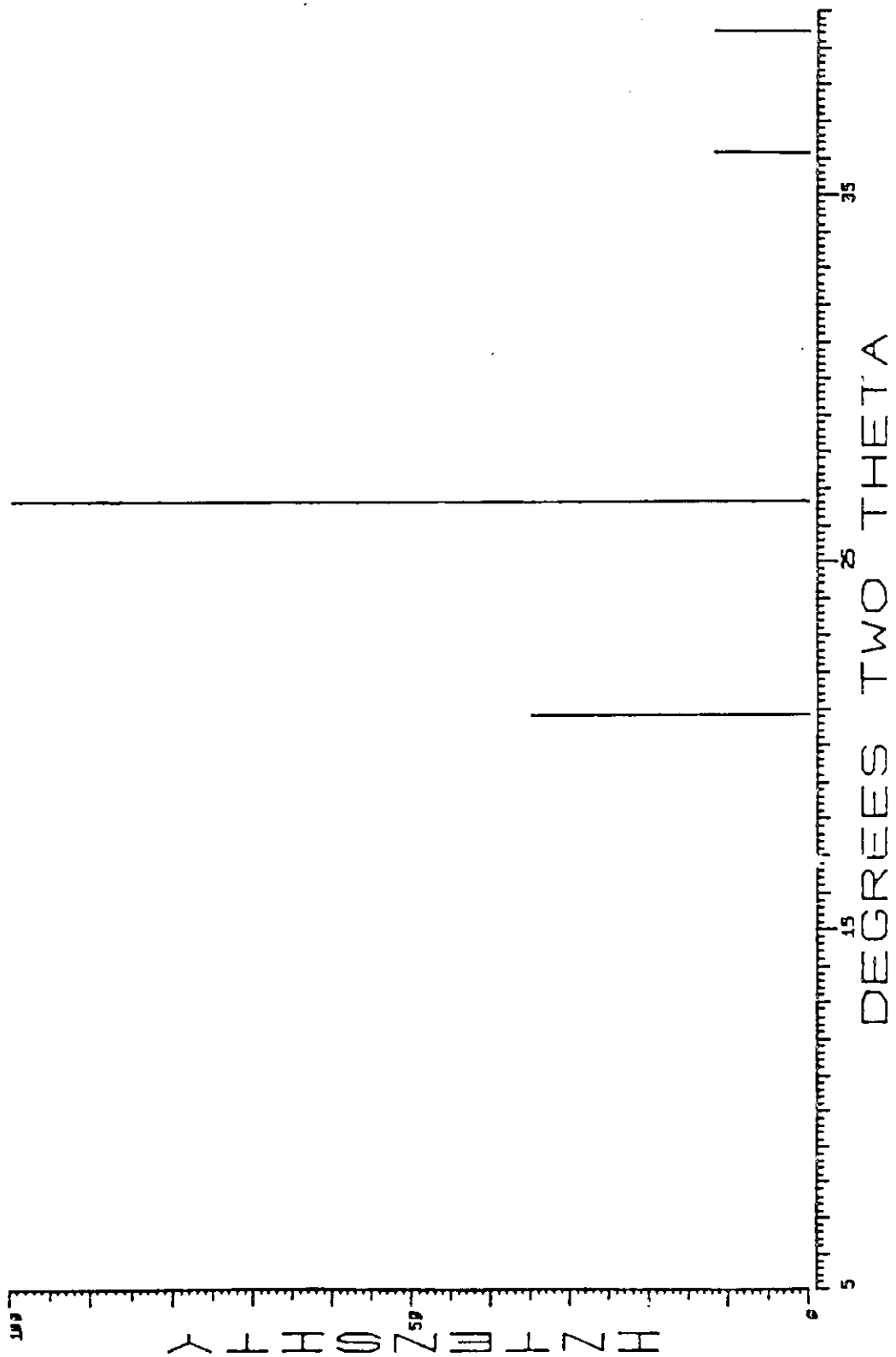

Figure 76. XRD Literature Line Pattern For Tridymite.

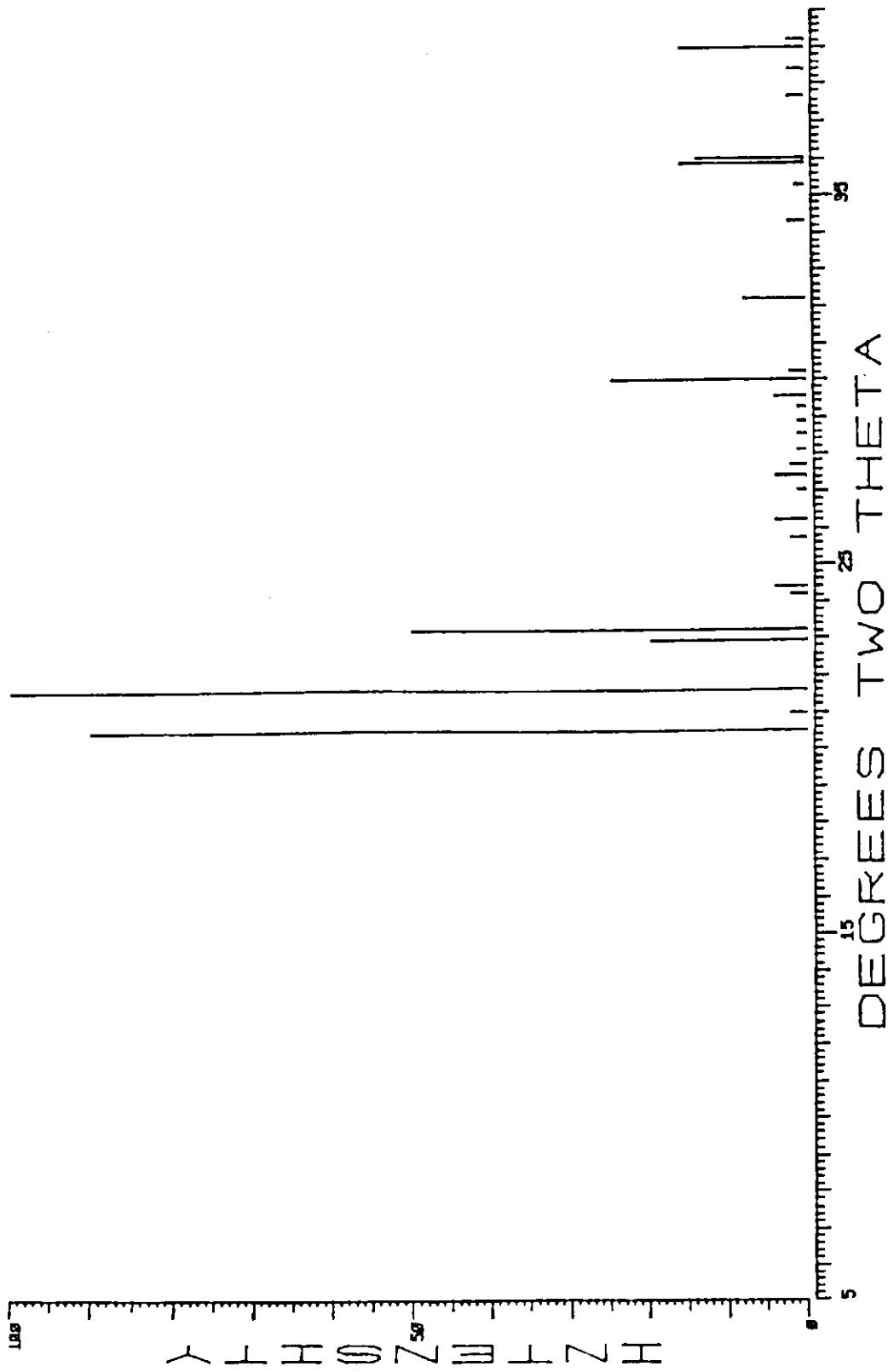

Figure 77. XRD Literature Line Pattern for ZSM-5.

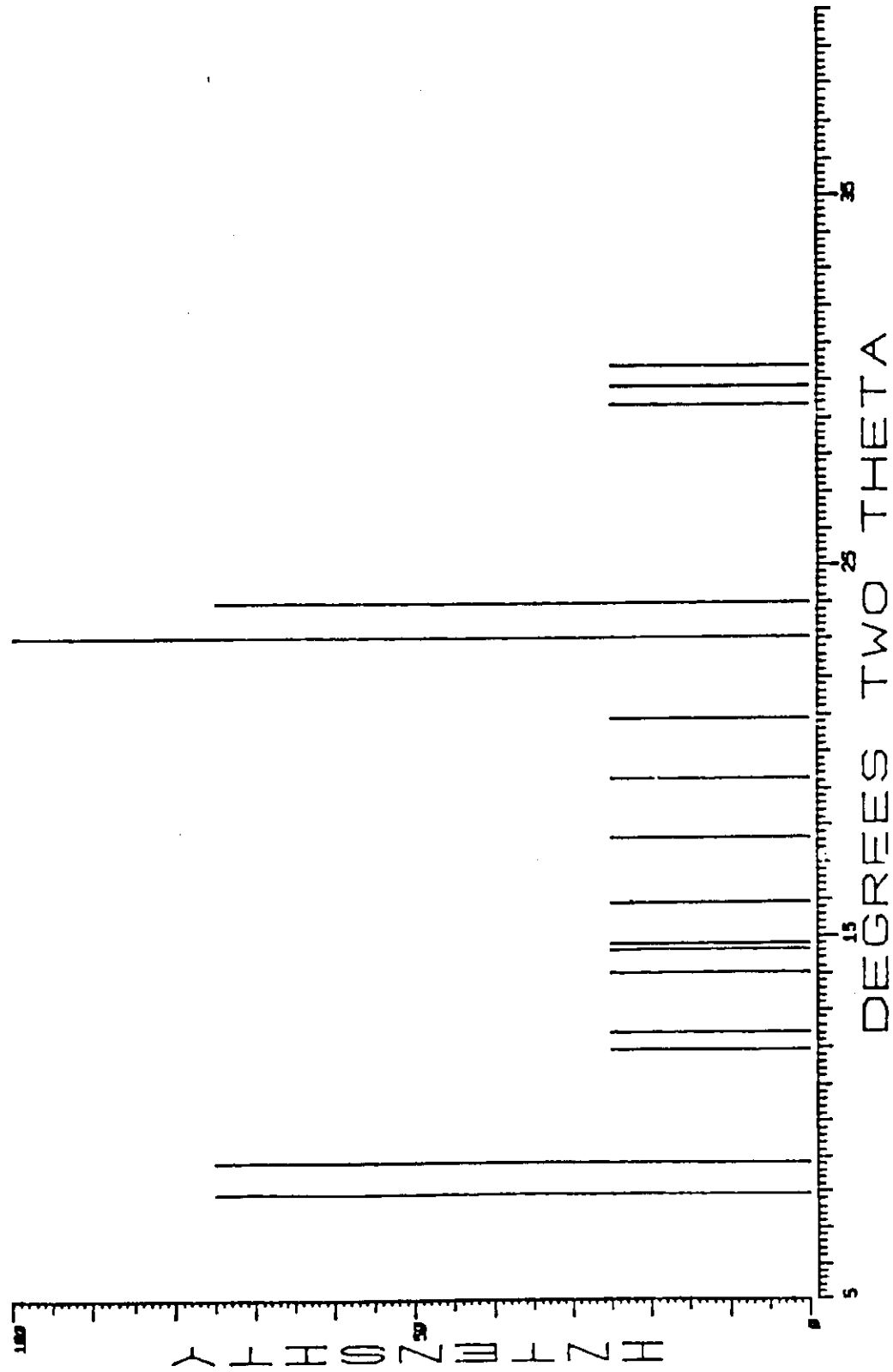

reported on page 10 of 0054386 0.1% Nu-5, 7.1% HZSM-5 might be explained as a slight reduction of the zeolite pore diameter due to carbon deposits or occluded species.